The zebrafish bcl-2 homologue Nrz controls development during somitogenesis and gastrulation via apoptosis-dependent and -independent mechanisms.

Estelle Arnaud, Kf Ferri, J. Thibaut, Z. Haftek-Terreau, A. Aouacheria, D. Leguellec, Thierry Lorca, G. Gillet

THE ZEBRAFISH BCL-2 HOMOLOGUE NRZ CONTROLS DEVELOPMENT DURING SOMITOGENESIS AND GASTRULATION VIA APOPTOSIS-DEPENDENT AND –INDEPENDENT MECHANISMS

Estelle ARNAUD[1, 4], Karine FERRI[1, *], Julien THIBAUT[1, *], Zofia TERREAU- HAFTEK[2, 5], Abdel AOUACHERIA[1, 6], Dominique LE GUELLEC[2], Thierry LORCA[3] and Germain GILLET[1, #]

[1]Apoptosis and Oncogenesis Laboratory , IBCP, UMR 5086 CNRS-UCBL, IFR 128, LYON France

[2]Extracellular Matrix and Development Laboratory, IBCP, UMR 5086 CNRS-UCBL, IFR 128, LYON France

[3]CRBM, UPR 1086 CNRS, route de Mende, 34293 Montpellier cedex 5, France

[4]Present address: Département de Biochimie, Université de Lausanne, Chemin de Boveresses 155, 1066 Epalinges, Switzerland

[5]Present address: Centre Intégratif de Génomique, Université de Lausanne, 1015 Lausanne-Dorigny, Switzerland

[6]Present address : Biométrie et Biologie Evolutive, UMR 5558 CNRS-UCB, 43 av du 11 novembre 69622 Villeurbanne cedex, France

[*] Equally contributing authors

[#] Corresponding author:

G. GILLET: Institut de Biologie et Chimie des Protéines, 7 passage du Vercors, 69367 Lyon cedex 07, France

e-mail: g.gillet@ibcp.fr

tel: (33) 4 72 72 26 01

fax: (33) 4 72 72 26 01

Running title: New Zebrafish Bcl-2 Homologue

ABSTRACT

Although the role of the Bcl-2 family of apoptosis inhibitors is well documented in tumor cells and tissue morphogenesis, their role during the early development of vertebrates is unknown. Here, we characterize Nrz, a new Bcl-2-related inhibitor of apoptosis in zebrafish. Nrz is a mitochondrial protein, antagonizing the death-accelerator Bax. The *nrz* gene is mainly expressed during gastrulation and somitogenesis. The knock-down of *nrz* with antisense morpholinos leads to alterations of the somites, correlated with an increase in apoptosis. In addition, earlier during development, in the zebrafish gastrula, *nrz* knock-down results in an increase of *snail-1* expression at the margin and frequent gastrulation arrest at the shield stage, independently of apoptosis. Together these data suggest that Nrz, in addition to its effect on apoptosis, contributes to cell movements during gastrulation by negatively regulating the expression of Snail-1, a transcription factor that controls cell adhesion.

Keywords: Apoptosis, Bcl-2, Gastrulation, Nr-13, Somites, Zebrafish

INTRODUCTION

Space and time-dependent control of programmed cell death (PCD) is essential for cell homeostasis in metazoans. Studies in nematode, drosophila and mouse have underscored the role of PCD in development (1), (2). In humans, deregulation of PCD is observed in degenerative diseases and cancer. Regulators of PCD are thus promising targets for drug discovery (3). The Bcl-2 family of proteins is critical for the control of PCD (4). These proteins control the release of cytochrome c from the mitochondria, a key step in apoptosis, the most documented type of PCD (4). Into the cell, they interact together, forming homo- or heterodimers; the relative concentrations of these complexes is critical for cell survival or death.

Interactions between Bcl-2 family members occur *via* conserved regions (5). Chemicals mimicking these interaction domains are used as decoy ligands to selectively inhibit the formation of such complexes (6). A number of these are being tested in preclinical or clinical trials (3). However all the interactions involving Bcl-2 family members are far from being characterized. Indeed, in addition to apoptosis, the Bcl-2 family plays numerous roles *e.g.* cell cycle control, genomic stability, cell signalling (7).

In vivo model systems are essential to study the various roles of this fascinating family of proteins in vertebrates. Among them, the zebrafish offers a number of advantages, *e.g.* rapid development, transparency of the embryo, genetic accessibility. The apoptosis machinery in the zebrafish is very similar to mammals. (8). In addition, the zebrafish develops a number of pathologies resembling human diseases, and is used for drug discovery projects (9).

We present the characterization of *nrz*, the zebrafish homologue of the chicken gene *nr-13*, a *bcl-2*-related gene involved in neoplastic transformation (10). In the embryo, the knock-down of *nrz* leads to an increase of apoptosis and affects somitogenesis. We also show here that, during gastrulation, the Nrz protein has apoptosis-independent effects and that the down-regulation of Nrz activates the expression of Snail-1, a transcription factor controlling the expression of cell adhesion molecules (11).

RESULTS AND DISCUSSION

Molecular cloning of nrz. Zebrafish EST clone # AW076878 exhibited the closest homology with the chicken antiapoptotic gene *nr-13*. The *nrz* gene exhibits one single intron at the same position as chicken *nr-13* and herpes virus (HVT) *vnr-13* (see supplementary data S1). This new gene was called *nrz,* for *nr-13* zebrafish.

The putative zebrafish protein deduced from the cDNA sequence exhibited the four typical Bcl-2 homology domains and the C-terminal hydrophobic tail, which characterize most apoptosis inhibitors. The sequence of the Nrz protein is highly homologous to chicken and HVT Nr-13 -39.7% and 38.7% identity, respectively- (Fig. 1), which identifies *nrz* as the orthologue of chicken *nr-13*. In contrast, the homology is significantly lower with the mammalian *nr-13* orthologues, namely human *nrh/bcl-b* (12), (13) and mouse *diva/boo* (14), (15). This suggests that in mammals the *nr-13* gene did evolve rapidly and may have acquired other functions, compared to egg-laying species.

Antiapoptotic activity of Nrz. The activity of the Nrz protein was evaluated *in vitro.* In *Xenopus* eggs extracts, Nrz was shown to delay caspase activation, acting as a Bax inhibitor (Fig. 2A). This result was confirmed using transient transfections. As shown in Fig. 2B, Nrz prevented cell death following serum withdrawal in Cos-7 cells. Taken together, these results show that Nrz is an apoptosis inhibitor and is presumably an antagonist of Bax.

A typical feature of Bcl-2-like proteins is their ability to interact with the outer mitochondrial membrane (16). Confocal microscopy analyses showed that Nrz is actually localized into the mitochondria, as Nr-13 itself and related apoptosis inhibitors (Fig. 2C). Together these results indicate that Nrz is a *bona fide* apoptosis inhibitor, acting at the mitochondrial level.

Expression of nrz during development. We examined *nrz* expression pattern during the development of the zebrafish by quantitative RT-PCR. The results in Fig. 3A show that the *nrz* transcript is present at 5 hours post fertilisation (hpf), corresponding to 50% epiboly. The *nrz* transcript is still present at 8 hpf (80% epiboly). At later stages, expression of *nrz* was mainly detected during late somitogenesis (20 hpf). *Nrz* expression was further analysed by whole mount *in situ* hybridization. In contrast to the sense riboprobe, which gave no signal (not shown), the antisense probe allowed to detect the *nrz* transcript. Zygotic expression was observed at 5-8 hpf, confirming RT-PCR data. During this period, corresponding to gastrulation and epiboly, the cells of the blastoderm move vegetally over the surface of the

yolk to envelop it completely. After the cells have covered about half of the yolk (50% epiboly) an involution process occurs throughout the margin of the epibolizing blastoderm, cells turning inward and moving back along the outer cell sheets. Remarkably, the *nrz* transcript was detected at the level of the yolk syncitial layer (YSL), mainly into the external YSL, close to the margin (Fig. 3B, 5 hpf). A typical ring shape labelling is observed as the margin gets closer to the vegetal pole (Fig. 3B, 8-10 hpf). At 18hpf, *i.e.* during myotome differentiation, *nrz* labelling was mainly detected in the somites, and to a lesser extent in the telencephalon (Fig. 3B, 18 hpf). Later on, *nrz* labelling gradually disappeared (not shown).

Nrz regulate apoptosis during somitogenesis. The role of *nrz* during development was further analysed using antisense oligonucleotides (morpholinos) designed to knock-down the expression of *nrz* at the translational level. FITC-labelled morpholinos were injected at the 1-4 cell stage and were found homogeneously distributed in the whole embryo at least for 48h (Fig. 4A). Two morpholinos were used: *nrz*-MO antisense, hybridizing at the vicinity of the AUG codon (see supplementary data S1), and 4mis-MO negative control. As shown in Fig. 4A, embryos injected with 4mis-MO behaved like non-injected embryos. In contrast, most embryos injected with the antisense (morphants) exibited major defects, particularly in the caudal region, as shown at 24 hpf (Fig. 4A, *nrz*-MO), see Table 1 (line 3: *nrz*-MO 250microM). In addition, morphants exhibited a high rate of mortality, 35% of the embryos dying before 10 hpf (n=247) when the *nrz*-MO morpholino was used at a concentration of 250 micromolar; mortality increased in a dose-dependent manner, reaching 85% at 1mM *nrz*-MO (n= 230), see Table 1. Remarkably, injection of *nrz*-MO in the YSL (where the *nrz* transcript is found) at 2.5 hpf (256 cells stage) significantly increased early mortality (51% at 250 micromolar, n=55). In contrast, 4mis-MO had no effect (5% mortality, n=149). Phenotype specificity of the morphants was confirmed by co-injecting the *in vitro* transcribed *nrz* mRNA together with *nrz*-MO. In these conditions, the phenotype of the injected embryos (95% normal, n=117) was the same as non-injected embryos (Fig 4A, *nrz*-MO+*nrz* mRNA). Coinjection of an unrelated mRNA did not rescue the phenotype of the morphants (35% mortality, n=50). We also checked the effect of injecting *nrz* mRNA alone: most corresponding embryos developed normally (85% normal, n=300), However early mortality was slightly increased (15%), compared to non injected embryos (5%), indicating that the overexpression of *nrz* might affect early development to some extent. Quantitative data are displayed in Table 1.

We directly evaluated the effect of *nrz*-MO on the amount of Nrz protein by Western blotting on whole embryo protein extracts. To this end, a rabbit polyclonal antibody was raised against the purified recombinant Nrz protein. As shown in Fig. 4B, *nrz*-MO down-regulated Nrz protein level, in contrast to 4mis-MO; co-injection of *nrz* mRNA, which maintained the Nrz concentration at normal levels, prevented the effect of *nrz*-MO.

These results confirmed that the phenotype of the morphants resulted from the knock-down of *nrz*. In these embryos, the somites were profoundly disorganized, with irregular boundaries and alterated expression of MyoD, a key transcription factor in muscle differentiation, Fig. 4C. Moreover, a number of cells of abnormal morphology accumulated, suggesting that there might have been an increase in cell death in the morphants. Indeed, a large number of TUNEL positive cells are detected in the morphants, compared to control embryos (Fig. 4D & 4E). Thus, in morphant embryos, the observed disorganization of the somites is correlated with increase of cell death. Of note, cell death is not only detected in the somites but also in other areas, including the head (Fig. 4E). This suggests that the control of apoptosis by Nrz might be crucial in a number of tissues during somitogenesis.

Nrz controls gastrulation independently of apoptosis. In addition to its effect on somitogenesis, we showed that *nrz* knock-down resulted in a significant increase in early mortality (up to 80%, depending on the concentration of the morpholino, compared to 5% for control embryos, see above and Table 1). Together with the fact that *nrz* was highly expressed during epiboly (Fig. 3), this suggested that *nrz* might also play a role before the onset of somitogenesis. Fig. 5 shows the typical behaviour of one morphant during the first 30 min following the shield stage (6 hpf). Whereas in normal embryos blastoderm cells continued to extend towards the vegetal pole (see Fig. 3B), this progression was stopped in a significant number of morphants at the shield stage (up to 80%), see Table 1. Then constriction of the embryo appeared at the margin. Cells at the margin eventually detached from the yolk in the shield area, and the entire embryo detached from the yolk within a few minutes. No such phenotype was observed with control embryos, indicating that this splitting off was actually due to *nrz* knock-down (Table 1). Although at this stage the apoptosis machinery did not yet seem to be in operation (17), we could not absolutely exclude that the knock-down of *nrz* would prematurely activate apoptosis, resulting in premature arrest of gastrulation. Actually, as shown in Fig. 6A, we found no increase of the number of TUNEL positive cells in embryos injected with *nrz*-MO. In addition, we analyzed whether apoptosis inhibitors acting downstream of *nrz* could rescue the « gastrulation arrest » phenotype. First, we used the pan

caspase inhibitor ZVAD-fmk, which efficiently inhibits caspase activation *in vivo* in the zebrafish embryo -not shown, see also (17)-. Regarding the effect of ZVAD-fmk on early mortality (10 hpf), which is a direct result of this premature gastrulation arrest, Fig. 6B shows that early mortality was not significantly affected by ZVAD-fmk in embryos injected with *nrz*-MO. Second, together with *nrz*-MO, we coinjected an antisense morpholino directed against the apoptosis accelerator Bax, which also failed to prevent the epiboly arrest due to *nrz* knock-down (Table 1). Together these results strongly suggested that the effect of *nrz* knock-down on gastrulation is apoptosis-independent. In contrast, ZVAD-fmk fully restores normal development of surviving morphants during somitogenesis (92% normal, see Table 1), confirming that, at these latter stages, the knock down of *nrz* activates caspase-dependent cell death.

Nrz controls gastrulation via a snail-1-dependent pathway. If not due to apoptosis, the cells may have detached as a consequence of modifications to their adhesion properties. Indeed, during gastrulation, important changes in cell adhesion and migration occur, some being collectively referred to as the epithelial-mesenchymal transition (EMT). The transcription Snail-1 regulates the expression of major adhesion proteins during gastrulation (18). We thus analysed the expression of *snail-1* by *in situ* hybridization in embryos expressing or not the Nrz protein. Remarkably, as shown in Fig. 7A, the expression level of *snail-1*, which is restricted to the margin, is significantly increased in the embryos injected with *nrz*-MO. These data were confirmed by quantitative RT-PCR. This suggested that *snail-1* is negatively regulated by Nrz. If *snail-1* acts downstream of *nrz*, one possibility could be that the overexpression of *snail-1* might lead to the same phenotype as *nrz* knock-down. Thus, the *in vitro* transcribed *snail-1* mRNA was injected into the embryos at the 1-4 cell stage and its effect on gastrulation was analyzed. Fig. 7B shows that the overexpression of *snail-1* mimics the effect of the *nrz*-MO antisense morpholino (40% «gastulation arrest» phenotype, n=295), indicating that *snail-1* may actually mediate the effect of *nrz* on cell adhesion during gastrulation. This hypothesis was confirmed by the fact that the knock-down of *snail-1* by coinjecting a *sna1*-MO antisense (referred to as *snail-1*-MO-1 in Table 1) together with *nrz*-MO rescued the gastrulation arrest phenotype observed at 6 hpf (98% normal, n=227), (Fig. 7C, Table 1). Coinjection of another *sna1*-MO antisense (referred to as *snail-1*-MO-2 in Table 1) had the same effect (82% normal, n=300), while the corresponding negative control 5mis-*snail-1*-MO-2 did not prevent the gastrulation arrest due to the knock down of *nrz* (36% gastrulation arrest, n=280), see Table 1.

During epiboly, *snail-1* is expressed in involuting cells of the germ ring at the margin of the blastoderm (19), (20). In contrast, according to our *in situ* hybridization data, the *nrz* transcript is present in the external YSL, at the vicinity of the germ ring. This suggests that Nrz may regulate *snail-1* gene expression non cell-autonomously. Indeed, direct injection of *nrz*-MO into the YSL at the 256 cells stage results in premature gastrulation arrest, which is prevented by first injecting *snail-1*-MO-1 or *snail-1*-MO-2, but not 5mis-*snail-1*-MO-2, at the 1-4 cell stage (Fig 7C, table 1).

Thus Nrz may control the release of inductive signals from the YSL which would in turn act on transduction pathways regulating *snail-1* expression in the embryo, such as those controlled by Notch or TGF BETA, two activators of *snail* expression and promoters of EMT as well (21), (22). However, on the basis of the result presented here one cannot exclude that *nrz* knock down might also affect gastrulation in a cell autonomous way, having direct effects in the YSL, which would in turn compromise adhesion between the yolk and the blastoderm. Indeed cell movements during gastrulation closely depend on cytoskeleton dynamics, which must be controlled very precisely (23). Actually, Bcl-2 itself might indirectly control microtubule dynamics via an Erk-dependent pathway, at least in certain cells (24). In addition, there is evidence for direct interactions between Bcl-2 family members and proteins of the cytoskeleton, or scaffold proteins, such as paxillin (25). Indeed, the Bcl-2 family appears to participate to multiple signalling pathways into the cell, independently of the apoptosis (26). This raises the possibility that Nrz may act on gastrulation *via* both non-cell and cell-autonomous mechanisms.

A number of genes involved in cell-cell or cell-matrix interactions, such as E-cadherin (27), fibronectin (18), collagen type II (28), appear to be regulated by the Snail family of transcription factors. Some of them regulate cell movements during early embryogenesis (29). These genes are potential targets of Bcl-2 family members, including Nrz. Actually, E-cadherin and collagen type II were reported to be regulated by Bcl-2, the canonical apoptosis inhibitor, (30), (31). Moreover, the knock down of E-cadherin strongly affects early development in the zebrafish (32). However, the knock down of *nrz* does not seem to affect the expression of E-cadherin in the zebrafish gastrula (results not shown), whereas paraxial protocadherin, another adhesion molecule having a role during gastrulation (33), is upregulated upon *nrz* knock down (see supplemental data S3). Thus, although the underlying molecular mechanisms remain to be determined, this report supports the idea that, during

development, cell movements and adhesion may be controlled by Bcl-2 family members, at least in part *via snail*-dependent pathways, independently of apoptosis.

MATERIALS AND METHODS

Zebrafish. Zebrafish (a cross between AB and Tübingen) were maintained under standard laboratory conditions (34). For some experiments ZVAD was added in the culture medium (300 μM final concentration) as described (35).

Nrz cloning. Databases were screened with chicken Nr-13 using tblastn. The AW076878 clone encoding a complete open reading frame was selected. The cDNA (531bp) corresponding to zebrafish nr-13 homologue (called nrz) was subcloned into pGEMT by PCR and entirely re-sequenced. Multialignments were performed with Clustal W and ESPript 2.2 softwares.

Nrz protein and antibody production. Nrz protein (residues 1-157) produced in BL-21(DE3) and purified as described previously (36), was used for polyclonal antibody production (Valbex, Villeurbanne). The rabbit antiserum was purified as described (10).

Caspase inhibition assay. Caspase inhibition assays in *Xenopus* egg extracts were performed as described (36). Briefly, *Xenopus* egg extracts were incubated with purified recombinant proteins Nrz or Nr-13, the latter used as a control, with or without the BH3-Bax peptide. At different time points, aliquots were incubated for 10 min. with 50 μM Ac-DEVD-AMC (Calbiochem). The reaction was stopped with cold PBS; cleavage of the caspase substrate Ac-DEVD-AMC was monitored with a FLX-800T (Bio-Teck) fluorimeter (excitation 380 nm, emission 460 nm).

Cell death assay in Cos-7 cells. *Nrz* cDNA was subcloned into the XhoI and SalI sites of pEGFP-C1(Clontech). Cos-7 cells were grown at 37°C, 5% CO_2 in DMEM medium supplemented with 10% foetal bovine serum. At 30% confluence, cells were transfected with pEGFP-C1-Nrz using Fugene 6 reagent as indicated by the manufacturers (Roche). Fourteen hours after transfection the media was replaced by DMEM without serum. Fourty eight hours after serum withdrawal, the percentage of transfected cells displaying pycnotic nuclei was measured using Hoechst 33258 fluorescent dye.

Confocal microscopy. Cells were incubated with Mitotracker™ (Molecular Probes) to visualise mitochondria as described (37). After four washes in PBS, cells were fixed with 4% paraformaldehyde for 20 min at room temperature and incubated 30 min with 5 µg/mL Hoechst 33258 to visualise nuclei. Cells were observed under a Leica TCS-SP2 confocal microscope.

Quantitative RT-PCR. Total RNA was extracted at different stages. Embryos were frozen in liquid nitrogen and homogenized in lysis buffer (4 M GIT, 25 mM sodium citrate, 0.5 % sarcosin, 1 % β-mercapto-ethanol) and extracted with phenol-chloroform. The aqueous phase was precipitated with 2 volumes of ethanol and 1/10 volume of 3M Na-acetate pH 5.3 and then purified by centrifugation in a CsCl gradient. Purified RNA was treated with RNase-free DNase, extracted with phenol-chloroform and resuspended in DEPC-treated water for reverse transcription.

Quantitative PCR were performed in triplicate using the Quantitect SYBR Green PCR kit (Qiagen) on an iCycler iQ (Biorad), using gene-specific primers for *nrz* (forward 5' AGCAGGAGTGGGTTTAGCTGGT; reverse 5' CAGCGCTGGGGAAAAAACAGTG), *sna-1* (forward 5' ACCTGCTCTCGCACCTTTAGT; reverse 5' TGATGCGTCATCCTTCTCCTG), and *histone 2A* (forward 5' CCTCGAGCTGGCCGGGAA; reverse 5' CTCGGACTAGCTGCGTTT), the latter being used for calibration.

Western blots. Total proteins were extracted from liquid nitrogen frozen embryos in RIPA buffer (1 % NP-40, 0.5% deoxycholic acid, 0.1% SDS in PBS) containing protease inhibitor cocktail (Roche). After protein concentration determination (Bradford's reagent), samples were loaded on 15 % acrylamide gels. Protein A-purified anti-Nrz antibody was used at 1/300 dilution.

In situ hybridization. *nrz* ORF was subcloned into the XhoI-SpeI sites of the pBIISK$^+$ vector to synthetize sense and antisense digoxygenin-labelled riboprobes. The *snail-1* probe was synthetized using the Snail-1/pB-SK$^+$ vector (19), a gift from B. Thisse. *In situ* hybridizations were performed as described (19).

TUNEL assays. Embryos were fixed in 4% paraformaldehyde in PBS overnight at 4 °C and stored in methanol at –20 °C. Assays were performed using in situ cell death detection kit (POD, Roche) as described by the manufacturers. Cell death was detected either using the

peroxydase reaction or by directly detecting the incorporated FITC-labelled nucleotides using a fluorescent microscope.

Morpholino and mRNA microinjection. Morpholinos were designed according to the manufacturer's recommendations (Gene Tools): *nrz*-MO 5'CATTTTCCTCCCAGCGATGTCAGAC hybridizes with *nrz* mRNA from position -22 to +3 relative to the start codon (see underlined sequence, Fig. 1). We used the same sequence with four mismatches (underlined) as negative control: 4mis-MO 5' CATTATCCTGCCAGCCATGTGAGAC. Except when TUNEL assays were subsequently carried out on injected embryos, morpholinos were labelled with fluorescein.

Other morpholinos: Bax antisense: *bax*-MO 5' CCACCCGACGGCGCTGCCATATTAG. Snail-1 antisense-1: *sna1*-MO-1 5' ATCAGTCCACTCCAGTTACTTTCAG (labelled with rhodamine). Snail-1 antisense-2: *sna1*-MO-2 5' GTCCACTCCAGTTACTTTCAGGGAT. Negative control (mismatches underlined): 5mis-*snail-1* MO-2 : 5'-GTCGAGTCCACTTAGTTTCACGGAT-3'.

Morpholinos were injected (5-10 nL) into 1-4 cell stage embryos at concentrations between 0.25 and 1mM in Danieau buffer (58 mM NaCl, 0.7 mM Kcl, 0.4 mM $MgSO_4$, 0.6 mM $Ca(NO_3)_2$, 5 mM Hepes pH 7.6).

Nrz and snail-1 ORFs were subcloned into the pCS_2^+ vector for *in vitro* transcription (SP6 mMESSAGE mMACHINE ^{TM} kit, Ambion). After Not1 linearization, reaction was performed using 1µg of plasmid template as indicated by the manufacturers. RNAs were micro-injected at a concentration of 100 ng/µL in nuclease free water.

ACKNOWLEDGEMENTS

We thank J. Gouttenoire, F. Mallein-Gerin and P. Blader for help and comments. B. Thisse is acknowledged for zebrafish probes. This work was supported by Retina France, the ARC the région Rhône-Alpes and the CNRS. EA was supported by the Ligue nationale contre le cancer. AA was supported by the CNRS and the FRM.

REFERENCES

1. Hengartner, MO. (1999) Programmed cell death in the nematode C. elegans. Recent Prog Horm Res 54: 213-222
2. Ranger, AM, Malynn, BA, and Korsmeyer, SJ. (2001) Mouse models of cell death. Nat Genet 28: 113-118
3. Reed, JC. (2003) Apoptosis-targeted therapies for cancer. Cancer Cell 3: 17-22
4. Scorrano, L, and Korsmeyer, SJ. (2003) Mechanisms of cytochrome c release by proapoptotic BCL-2 family members. Biochem Biophys Res Commun 304: 437-444
5. Gross, A, McDonnell, JM, and Korsmeyer, SJ. (1999) BCL-2 family members and the mitochondria in apoptosis. Genes Dev 13: 1899-1911
6. Moreau, C, Cartron, PF, Hunt, A, Meflah, K, Green, DR, Evan, G, Vallette, FM, and Juin, P. (2003) Minimal BH3 peptides promote cell death by antagonizing anti-apoptotic proteins. J Biol Chem 278: 19426-19435
7. Bonnefoy-Berard, N, Aouacheria, A, Verschelde, C, Quemeneur, L, Marcais, A, and Marvel, J. (2004) Control of proliferation by Bcl-2 family members. Biochim Biophys Acta 1644: 159-168
8. Inohara, N, and Nunez, G. (2000) Genes with homology to mammalian apoptosis regulators identified in zebrafish. Cell Death Differ 7: 509-510
9. Pichler, FB, Laurenson, S, Williams, LC, Dodd, A, Copp, BR, and Love, DR. (2003) Chemical discovery and global gene expression analysis in zebrafish. Nat Biotechnol 21: 879-883
10. Gillet, G, Guerin, M, Trembleau, A, and Brun, G. (1995) A Bcl-2-related gene is activated in avian cells transformed by the Rous sarcoma virus. Embo J 14: 1372-1381
11. Locascio, A, Manzanares, M, Blanco, MJ, and Nieto, MA. (2002) Modularity and reshuffling of Snail and Slug expression during vertebrate evolution. Proc Natl Acad Sci U S A 99: 16841-16846
12. Aouacheria, A, Arnaud, E, Venet, S, Lalle, P, Gouy, M, Rigal, D, and Gillet, G. (2001) Nrh, a human homologue of Nr-13 associates with Bcl-Xs and is an inhibitor of apoptosis. Oncogene 20: 5846-5855
13. Ke, N, Godzik, A, and Reed, JC. (2001) Bcl-B, a novel Bcl-2 family member that differentially binds and regulates Bax and Bak. J Biol Chem 276: 12481-12484
14. Inohara, N, Gourley, T, Carrio, R, Muniz, M, Merino, J, Garcia, I, Koseki, T, Hu, Y, Chen, S, and Nunez, G. (1998) Diva, a Bcl-2 Homologue that Binds Directly to Apaf-1 and Induces BH3-independent Cell Death. J. Biol. Chem. 273: 32479-32486
15. Song, Q, Kuang, Y, Dixit, VM, and Vincenz, C. (1999) Boo, a novel negative regulator of cell death, interacts with Apaf-1. Embo J 18: 167-178
16. Green, DR, and Kroemer, G. (2004) The pathophysiology of mitochondrial cell death. Science 305: 626-629
17. Ikegami, R, Hunter, P, and Yager, TD. (1999) Developmental activation of the capability to undergo checkpoint-induced apoptosis in the early zebrafish embryo. Dev Biol 209: 409-433
18. Nieto, MA. (2002) The snail superfamily of zinc-finger transcription factors. Nat Rev Mol Cell Biol 3: 155-166
19. Thisse, C, Thisse, B, Schilling, TF, and Postlethwait, JH. (1993) Structure of the zebrafish snail1 gene and its expression in wild-type, spadetail and no tail mutant embryos. Development 119: 1203-1215
20. Hammerschmidt, M, and Nusslein-Volhard, C. (1993) The expression of a zebrafish gene homologous to Drosophila snail suggests a conserved function in invertebrate and vertebrate gastrulation. Development 119: 1107-1118

21. Timmerman, LA, Grego-Bessa, J, Raya, A, Bertran, E, Perez-Pommares, JM, Diez, J, Aranda, S, Palomo, S, McCormick, F, Izpisua-Belmonte, JC, and de la Pompa, JL. (2004) Notch promotes epithelial-mesenchymal transition during cardiac development and oncogenic transformation. Genes Dev 18: 99-115
22. Peinado, H, Quintanilla, M, and Cano, A. (2003) Transforming growth factor beta-1 induces snail transcription factor in epithelial cell lines: mechanisms for epithelial mesenchymal transitions. J Biol Chem 278: 21113-21123
23. Solnica-Krezel, L, and Driever, W. (1994) Microtubule arrays of the zebrafish yolk cell: organization and function during epiboly. Development 120: 2443-2455
24. Jiao, J, Huang, X, Feit-Leithman, RA, Neve, RL, Snider, W, Dartt, DA, and Chen, DF. (2005) Bcl-2 enhances Ca(2+) signaling to support the intrinsic regenerative capacity of CNS axons. Embo J 24: 1068-1078
25. Sorenson, CM. (2004) Interaction of bcl-2 with Paxillin through its BH4 domain is important during ureteric bud branching. J Biol Chem 279: 11368-11374
26. Reed, JC. (1998) Bcl-2 family proteins. Oncogene 17: 3225-3236
27. Hemavathy, K, Ashraf, SI, and Ip, YT. (2000) Snail/slug family of repressors: slowly going into the fast lane of development and cancer. Gene 257: 1-12
28. Seki, K, Fujimori, T, Savagner, P, Hata, A, Aikawa, T, Ogata, N, Nabeshima, Y, and Kaechoong, L. (2003) Mouse Snail family transcription repressors regulate chondrocyte, extracellular matrix, type II collagen, and aggrecan. J Biol Chem 278: 41862-41870
29. Ettensohn, CA. (1999) Cell movements in the sea urchin embryo. Curr Opin Genet Dev 9: 461-465
30. Kinkel, MD, and Horton, WE, Jr. (2003) Coordinate down-regulation of cartilage matrix gene expression in Bcl-2 deficient chondrocytes is associated with decreased SOX9 expression and decreased mRNA stability. J Cell Biochem 88: 941-953
31. Li, L, Backer, J, Wong, AS, Schwanke, EL, Stewart, BG, and Pasdar, M. (2003) Bcl-2 expression decreases cadherin-mediated cell-cell adhesion. J Cell Sci 116: 3687-3700
32. Kane, DA, McFarland, KN, and Warga, RM. (2005) Mutations in half baked/E-cadherin block cell behaviors that are necessary for teleost epiboly. Development 132: 1105-1116
33. Yamamoto, A, Amacher, SL, Kim, SH, Geissert, D, Kimmel, CB, and De Robertis, EM. (1998) Zebrafish paraxial protocadherin is a downstream target of spadetail involved in morphogenesis of gastrula mesoderm. Development 125: 3389-3397
34. Westerfield, M. (2000) *The zebrafish book*, University of Oregon Press, Eugene, OR
35. Williams, JA, Barrios, A, Gatchalian, C, Rubin, L, Wilson, SW, and Holder, N. (2000) Programmed cell death in zebrafish rohon beard neurons is influenced by TrkC1/NT-3 signaling. Dev Biol 226: 220-230
36. Moradi-Ameli, M, Lorca, T, Ficheux, D, di Pietro, A, and Gillet, G. (2002) Interaction between the antiapoptotic protein Nr-13 and cytochrome c. Antagonistic effect of the BH3 domain of Bax. Biochemistry 41: 8540-8550
37. Aouacheria, A, Ory, S, Schmitt, JR, Rigal, D, Jurdic, P, and Gillet, G. (2002) p60(v-src) and serum control cell shape and apoptosis via distinct pathways in quail neuroretina cells. Oncogene 21: 1171-1186

LEGENDS TO FIGURES

Figure 1. Sequence of the Nrz protein. *Alignment of Nrz with chick Nr-13 (AAK54806), HVT vNr-13 (AY756568), human Nrh (AJ458330) and mouse Diva/Boo (AAC83150).* Identical and similar amino acids are boxed in dark and light grey respectively. Positions of BH domains and of the C-terminal hydrophobic domain (TM) are shown.

Figure 2. Anti-apoptotic activity and subcellular localization of Nrz. *A . Inhibition of caspase activation*. *Xenopus* eggs extracts were incubated in the presence of buffer alone, BH3-Bax peptide (corresponding to the BH3 domain of Bax), chicken Nr-13, zebrafish Nrz either alone or with BH3-Bax. At indicated times, caspase activity was measured by fluorimetry. Nrz and Nr-13 both inhibit caspase activity. Nrz is an inhibitor of BH3-Bax. Representative results of three independent experiments.

B. Nrz inhibits cell death in vertebrate cells. Cos-7 cells were transfected either by the empty vector (pEGFP-C1) or the recombinant vector (pEGFP-C1/nrz), expressing GFP and GFP-Nrz fusion protein, respectively. Cells were grown for 48h with (+) or without (-) serum. Percentage of apoptotic cells was estimated by counting pycnotic nuclei in transfected cells (GFP positive), using a fluorescence microscope. Results of two independent experiments carried out in triplicate; standard error of the mean is shown.

C. Nrz is a mitochondrial protein. Analysis of Nrz subcellular localization by confocal microscopy. Cos-7 cells were transiently transfected with pEGFP-C1 or pEGFP-C1/nrz expressing GFP or GFP-Nrz fusion protein, respectively. Mitochondria and nuclei were visualised using Mitotracker^{TM} Red and Hoechst 33258, respectively. In contrast to GFP, the GFP-Nrz protein colocalizes with Mitotracker^{TM}.

Figure 3. *nrz* expression in the embryo. *A. Quantitative RT-PCR*. Histograms represent signal intensity ratio (arbitrary units) between Nrz and histone H2A, used for calibration. Experiment performed on total RNAs prepared from whole embryos. Results of two independent experiments carried out in triplicate. Standard error of the mean is shown.

B. Whole mount in situ hybridization. At the 50% epiboly stage (5 hpf), *nrz* is expressed in the yolk syncytial layer (YSL); (a), side view, showing expression in both the internal YSL (I-YSL) and the external YSL (E-YSL); (b), vegetal view, showing expression in the I-YSL; (c), animal view. Expression in the E-YSL is maintained throughout the whole epiboly process (8-10 hpf). Later on (18 hpf, a, b), *nrz* expression is detected in the somites (S) and the telencephalon (T). Cross-section shows *nrz* transcript in the myotome (18 hpf, c).

Figure 4. Effect of knock-down of *nrz* on somitogenesis. *A. Detection of FITC-labelled morpholinos in 24 hpf zebrafish embryos*. Injected embryos are fluorescent. Non-injected embryo is shown (left panel). Embryos injected with the negative control 4mis-MO are normal (middle left panel). In contrast, embryos injected with the antisense morpholino *nrz*-MO are disorganized in the caudal region (middle right panel). Coinjection of the *nrz* mRNA together with *nrz*-MO restores wild type phenotype (right panel).

B. Detection of the Nrz protein. Whole protein extracts from zebrafish embryos (5 hpf) were analysed by western blot using the polyclonal anti-Nrz antibody or the pre-immune serum. Negative control (4mis), antisense (*nrz*-MO), antisense together with *in vitro* synthetized *nrz* mRNA (*nrz*-MO + mRNA *nrz*), *in vitro* transcribed *nrz* mRNA alone (mRNA *nrz*).

Top: a signal is detected at 16.kD with the anti-Nrz antibody, but not by the preimmune serum, corresponding to the predicted molecular weight of the Nrz protein. This band disappears upon injection of the Mo-*nrz* morpholino. Overexposure of the western blot (left lanes: exposure time 15 minutes) reveals a non specific band at 26kD (star) which is detected both by the preimmune serum and the anti-Nrz antibody. Embryos injected with the *in vitro* transcribed *nrz* mRNA accumulate large amounts of the Nrz protein (right lanes, exposure time 1 min). In these experiments, the non specific signal at 26kD is used as internal loading control.

Bottom: Coomassie blue staining of the protein samples electrophoresed in parallel on a second gel in exactly the same conditions, for quality control.

C. Phenotype of injected embryos 16 hpf. Somites are disorganised in embryos injected with the antisense (*nrz*-MO), but not with the negative control (4mis-MO). Top panels, low

magnification; middle panels, high magnification (Nomarski); bottom panel, detection of *myoD* expression (in situ hybridization). Injection of *nrz*-MO results in the appearance of apoptotic cells (upper & middle right panels, arrows). Somite boundaries are irregular (middle right), *myoD* expression pattern is drastically altered (bottom right).

D. Effect of nrz knock-down on cell death at 16 hpf. Cell death was detected by TUNEL assay at 16 hpf. Pictures were taken after completion of the peroxydase reaction. Embryos were injected with the negative control (4mis-MO, left panel) or the antisense (*nrz*-MO, right panel). The *nrz*-MO-injected embryo is TUNEL positive.

E. Effect of nrz knock-down on cell death at 23hpf. Cell death was detected by TUNEL assay at 23 hpf. In this case embryos were observed under the fluorescent microscope to directly detect incorporated FITC-labelled nucleotides. Embryos injected with *nrz*-MO, (bottom), but not the 4mis negative control (top, right) are fluorescent and thus TUNEL positive. Whole embryo is shown (bottom right), except the tail, which is out of focus. The tail is shown at higher magnification on the next panel (bottom left). Side view of positive control is shown (DNAse I-treated embryo, top right). In this experiment, the negative control is overexposed, a non specific signal is observed into the vitellus.

Figure 5. Effect of the knock-down of *nrz* on gastrulation. Video time lapse analysis of morphant embryos. The video sequence shown starts at the 50% epiboly stage (time 0). Progression of the margin is arrested (0-13'). Cells begin to detach in the area of the shield (21', arrow). Cells of the hypoblast detach from the yolk syncitial layer (23-25'). The embryo falls apart (26-27').

Figure 6. Apoptosis-independent effect of *nrz* knock-down on gastrulation. *A. Detection of cell death (shield stage).* Embryos injected with negative control (4mis-MO) and antisense morpholino (*nrz*-MO) are both TUNEL negative.

B. Early mortality due to nrz knock-down is caspase-independent. Injected embryos (with 4mis-MO or *nrz*-MO) were treated or not by ZVAD. Histograms represent percentage of mortality at 10 hpf. Results of three independent experiments carried out in duplicate. Standard error of the mean is shown.

Figure 7. Interplay between Nrz and Snail-1 during gastrulation.

A. *nrz knock–down increases the expression level of snail-1 in the margin*. Embryos were observed at 6hpf. Top panels: whole mount *in situ* analysis of *snail-1* expression in embryos injected with the negative control (4mis-MO, left) or antisense morpholino (*nrz*-MO, right). Bottom panel: quantitative RT PCR analysis of total *snail* mRNA amount in zebrafish extracts (arbitrary units). wt: non-injected embyos; *nrz*-MO: embryos injected with the antisense morpholino, representative result of three independent experiments.

B. The ectopic expression of snail-1 mimics the phenotype of nrz knock-down. Embryos (1-4 cell stage) were injected with the negative control (4mis-MO, left panel), the antisense morpholino (*nrz*-MO, middle panel) or the *in vitro* synthetized *snail-1* mRNA (right). Embryos shown in the middle and right panels are similar. Time lapse video recording of a *sna1* morphant is shown as supplementary data (S2).

C. Down regulation of Snail-1 rescues the gastrulation arrest phenotype. Embryos are observed at 50% epiboly (left) and 80% epiboly (right) and injected either at 1-4 cell stage (upper panels "*snail1*-MO" and middle panels) or at the 256 cells stage (bottom panels). Upper left panel, non-injected embryo (wt). Middle left panel, embryos injected with the *nrz*-MO antisense morpholino exhibit abnormal gastrulation. Whereas *snail-1* antisense *sna1*-MO has no effect (upper panels "*snail1*-MO"), Coinjection of *sna1*-MO together with *nrz*-MO restores normal gastrulation (middle panels "*nrz*-MO + *snail1*-MO"). *Nrz*-MO and *sna1*-MO are labelled in green and red, respectively; embryos injected with both morpholinos at 1-4 cell stage appear in yellow (middle panels). Direct injection of *nrz*-MO (green) in the YSL also results in premature gastrulation arrest (bottom panels "*nrz*-MO late"), which is fully prevented by first injecting *sna1*-MO (red) in the animal pole at 1-4 cells stage (bottom panels, "*nrz*-MO late + *snail1*-MO").

Injections	Number of embryos (n)	Phenotypes (50% epiboly)	Early mortality (10 hpf)	Phenotypes (16 – 24 hpf)
Non injected	200	100% normal	5%	95% normal
4mis-MO	149	100% normal	5%	95% normal
nrz-MO (250microM)	247	30% gastrulation arrest	35%	98% abnormal somites
nrz-MO (333microM)	640	50% gastrulation arrest	55%	
nrz-MO (1mM)	230	80% gastrulation arrest	85%	
nrz-MO (250microM) + Z-VAD.fmk	35	29% gastrulation arrest	35%	92% normal
nrz-MO (250microM) + *bax*-MO (250 microM)	64	30% gastrulation arrest		
nrz-MO (250microM) + *nr-13* mRNA	117	100% normal	5%	
nrz-MO (250microM) + non relevant mRNA	50	30% gastrulation arrest	35%	
nrz mRNA	300	90% normal	15%	90% normal
nrz-MO (250microM)+ *snail-1*-MO-1	227	98% normal	7%	
nrz-MO (333microM)+ *snail-1*-MO-2	300	82% normal		
nrz-MO (333microM)+ 5mis-*snail-1*-MO-2	280	36% gastrulation arrest		
snail-1-MO-1	48	98% normal	5%	
snail-1-MO-2	150	100% normal	5%	
nrz-MO (250microM at 2.5hpf)	55	51% gastrulation arrest	56%	
nrz-MO (333microM at 2.5hpf)	250	62% gastrulation arrest	67%	
nrz-MO (250microM at 2.5hpf) + *snail-1*-MO-1 (1-4 cell)	350	100% normal	5%	
nrz-MO (333microM at 2.5hpf) + *snail-1*-MO-1 (1-4 cell)	250	100% normal	5%	
nrz-MO (333microM at 2.5hpf) + *snail-1*-MO-2 (1-4 cell)	180	77% normal	82%	
nrz-MO (333microM at 2.5hpf) + 5mis-*snail-1*-MO-2 (1-4 cell)	130	50% gastrulation arrest	55%	
snail-1 mRNA	295	40% gastrulation arrest	45%	

Table I. Effect of morpholinos on early development of zebrafish embryos. Injections performed at the 1-4 cell stage, except if otherwise indicated. Concentration of injected morpholinos was 1mM, except when otherwise indicated (brackets). *In vitro* transcribed mRNAs were all used at 100ng/microliter. To assess specificity, two *snail-1* antisense morpholinos were used (*snail-1*-MO-1 & -2) as well as a negative control with five mismatches (5mis-*snail-1*-MO-2).

Injections	Number of embryos (n)	Phenotypes (50% epiboly)	Early mortality (10 hpf)	Phenotypes (16 – 24 hpf)
Non injected	200	100% normal	5%	95% normal
4mis-MO	149	100% normal	5%	95% normal
nrz-MO (250microM)	247	30% gastrulation arrest	35%	98% abnormal somites
nrz-MO (333microM)	640	50% gastrulation arrest	55%	
nrz-MO (1mM)	230	80% gastrulation arrest	85%	
nrz-MO (250microM) + Z-VAD.fmk	35	29% gastrulation arrest	35%	92% normal
nrz-MO (250microM) + *bax*-MO (250 microM)	64	30% gastrulation arrest		
nrz-MO (250microM) + *nr-13* mRNA	117	100% normal	5%	
nrz-MO (250microM) + non relevant mRNA	50	30% gastrulation arrest	35%	
nrz mRNA	300	90% normal	15%	90% normal
nrz-MO (250microM)+ *snail-1*-MO-1	227	98% normal	7%	
nrz-MO (333microM)+ *snail-1*-MO-2	300	82% normal		
nrz-MO (333microM)+ 5mis-*snail-1*-MO-2	280	36% gastrulation arrest		
snail-1-MO-1	48	98% normal	5%	
snail-1-MO-2	150	100% normal	5%	
nrz-MO (250microM at 2.5hpf)	55	51% gastrulation arrest	56%	
nrz-MO (333microM at 2.5hpf)	250	62% gastrulation arrest	67%	
nrz-MO (250microM at 2.5hpf) + *snail-1*-MO-1 (1-4 cell)	350	100% normal	5%	
nrz-MO (333microM at 2.5hpf) + *snail-1*-MO-1 (1-4 cell)	250	100% normal	5%	
nrz-MO (333microM at 2.5hpf) + *snail-1*-MO-2 (1-4 cell)	180	77% normal	82%	
nrz-MO (333microM at 2.5hpf) + 5mis-*snail-1*-MO-2 (1-4 cell)	130	50% gastrulation arrest	55%	
snail-1 mRNA	295	40% gastrulation arrest	45%	

Table I. Effect of morpholinos on early development of zebrafish embryos. Injections performed at the 1-4 cell stage, except if otherwise indicated. Concentration of injected morpholinos was 1mM, except when otherwise indicated (brackets). *In vitro* transcribed mRNAs were all used at 100ng/microliter. To assess specificity, two *snail-1* antisense morpholinos were used (*snail-1*-MO-1 & -2) as well as a negative control with five mismatches (5mis-*snail-1*-MO-2).

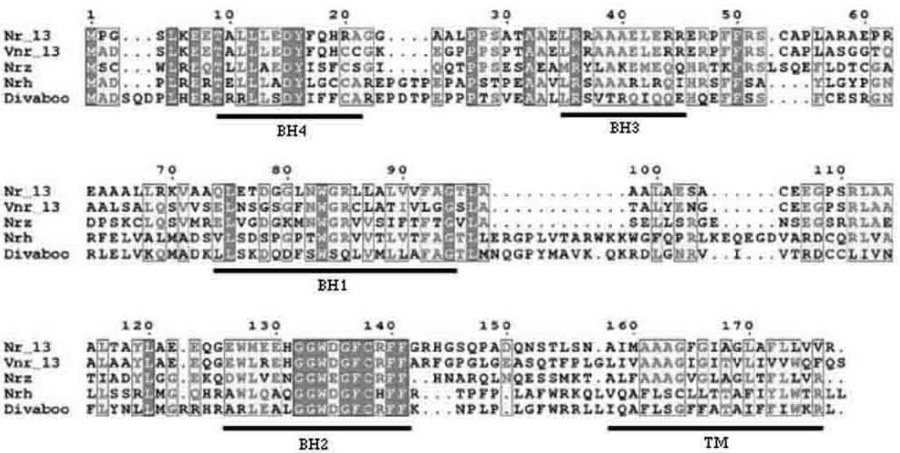
Nr_13
Vnr_13
Nrz
Nrh
Divaboo
BH4
BH3
BH1
BH2
TM

A

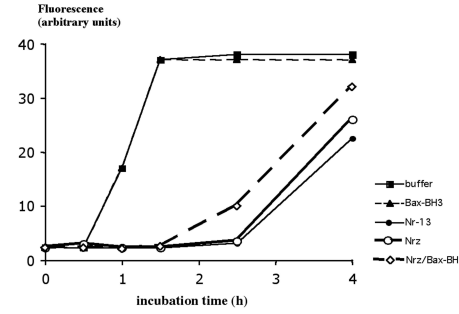
Fluorescence
(arbitrary units)
40
30
20
10
0
0
1
2
3
4
incubation time (h)
buffer
Bax-BH3
Nr-13
Nrz
Nrz/Bax-BH3

B

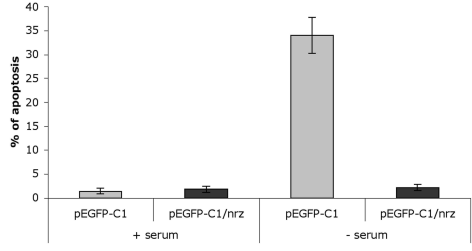
% of apoptosis
40
35
30
25
20
15
10
5
0
pEGFP-C1
pEGFP-C1/nrz
pEGFP-C1
pEGFP-C1/nrz
+ serum
- serum

C

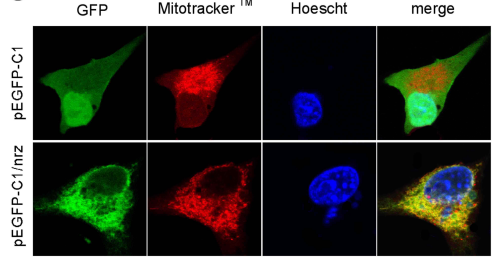
GFP
Mitotracker IM
Hoescht
merge
pEGFP-C1
pEGFP-C1/nrz

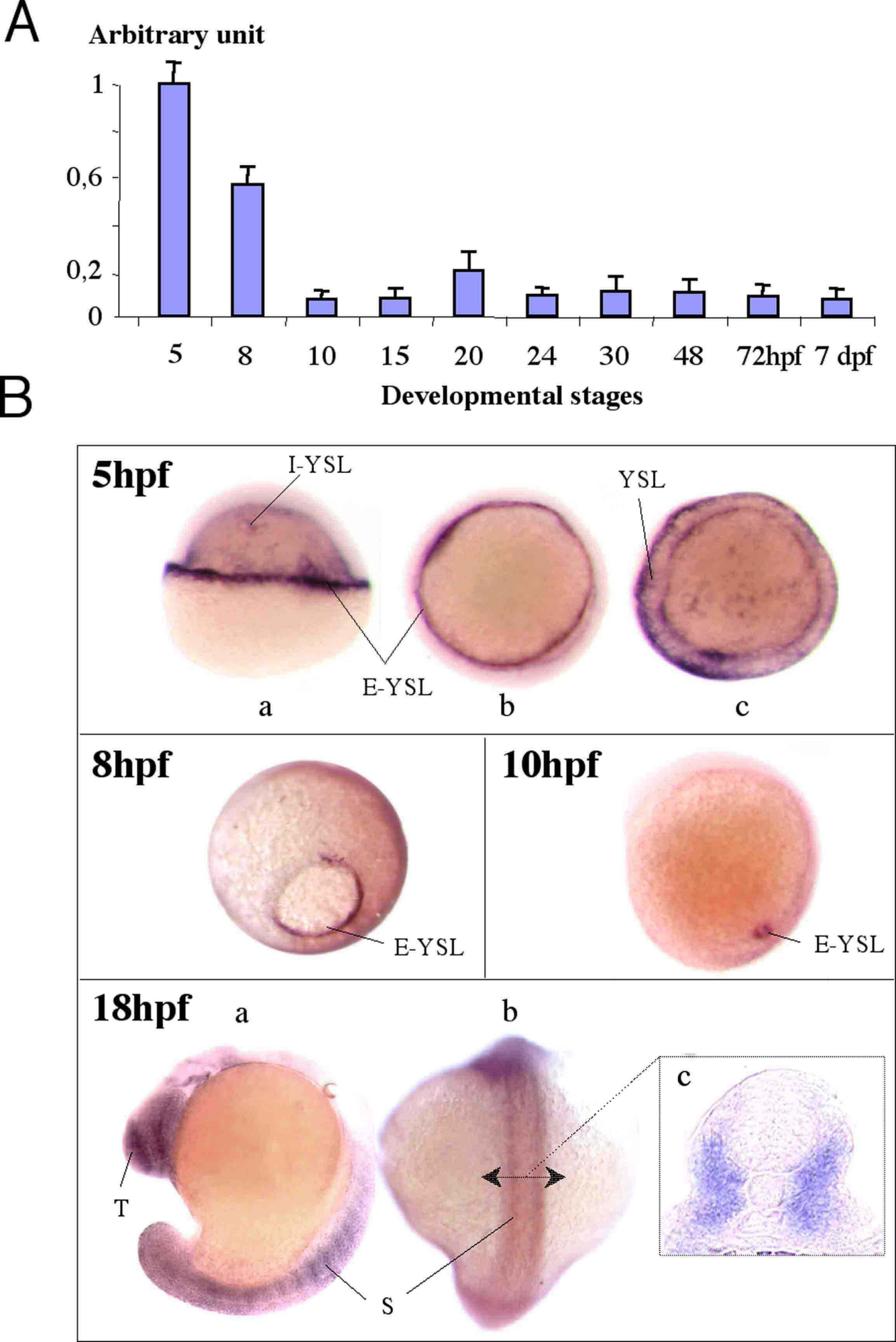
A
Arbitrary unit
1
0,6
0,2
0
5
8
10
15
20
24
30
48
72hpf
7 dpf
Developmental stages
B
5hpf
I-YSL
YSL
E-YSL
a
b
c
8hpf
E-YSL
10hpf
E-YSL
18hpf
a
b
c
T
S

A

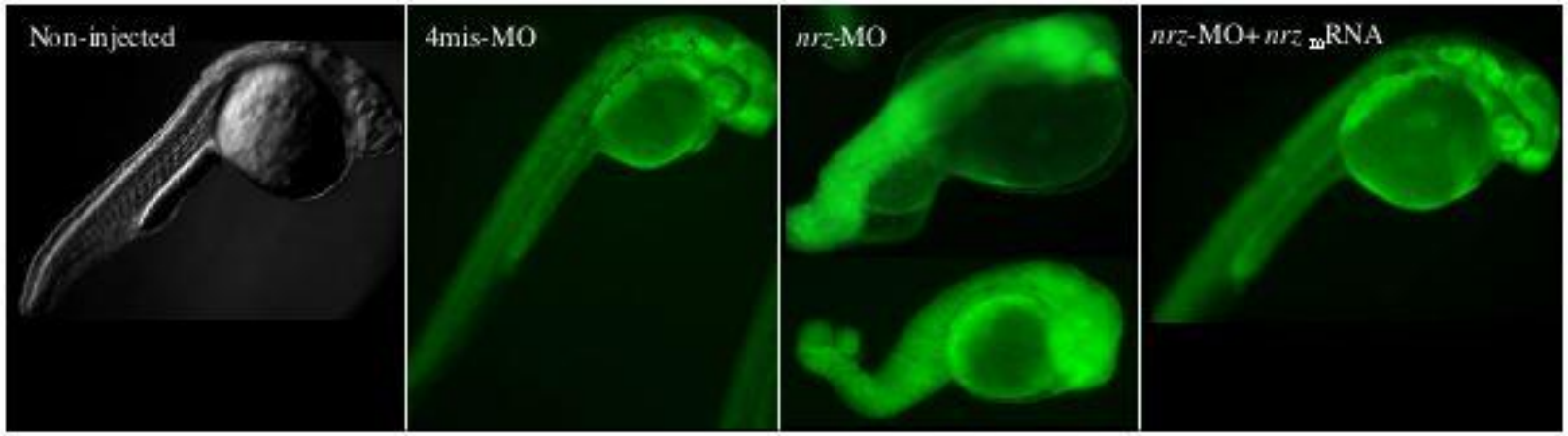

Figure 4A

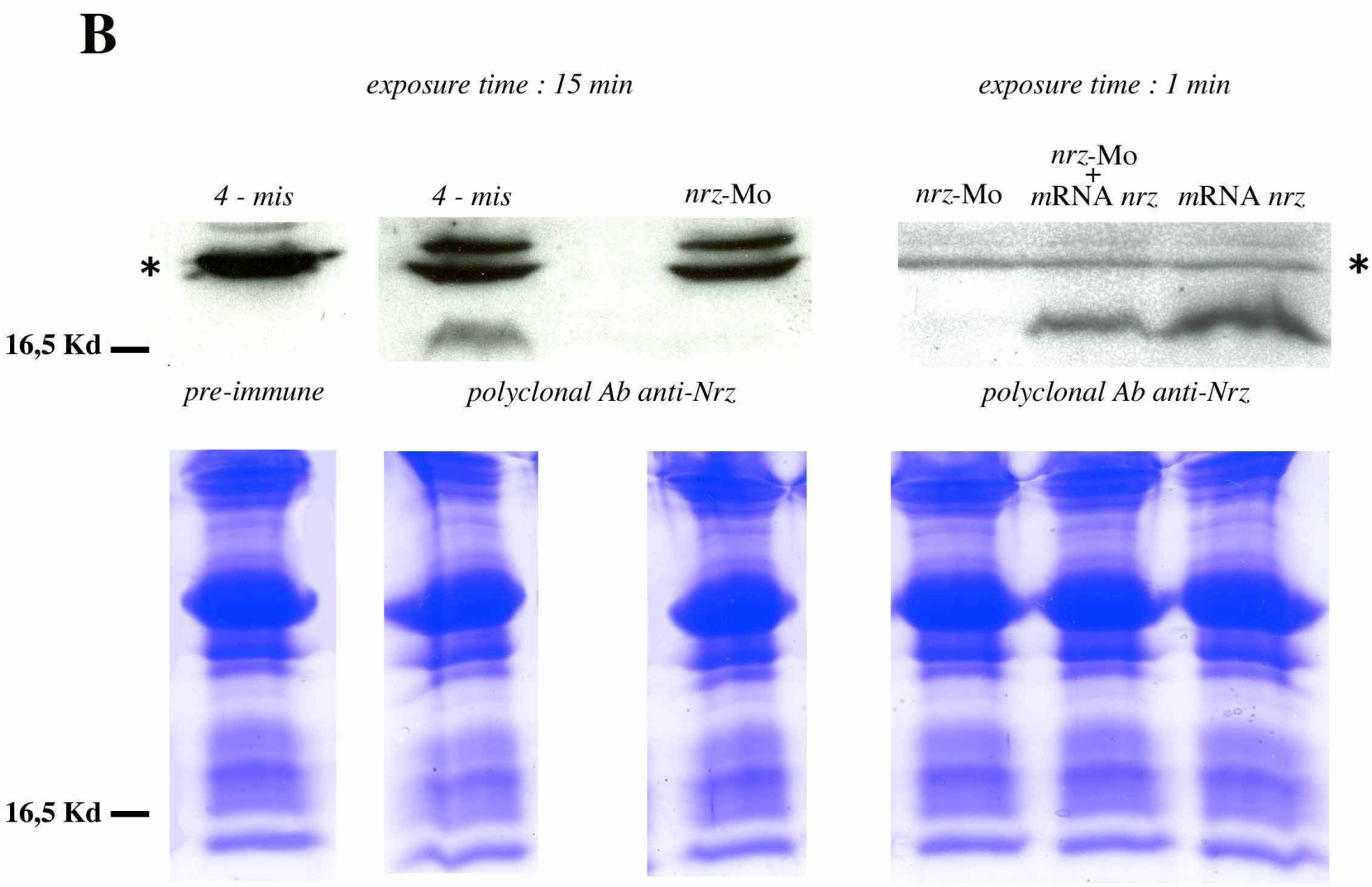
B
exposure time : 15 min
exposure time : 1 min
4 - mis
4 - mis
nrz-Mo
nrz-Mo
nrz-Mo
+
mRNA nrz
mRNA nrz
*
*
16,5 Kd
pre-immune
polyclonal Ab anti-Nrz
polyclonal Ab anti-Nrz
16,5 Kd

Figure 4B

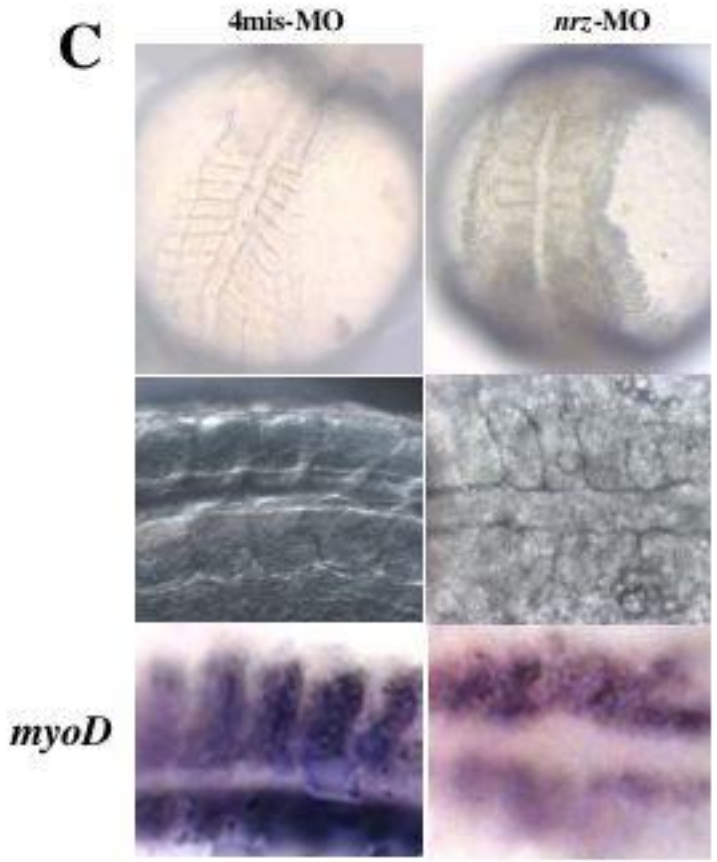

Figure 4C

D

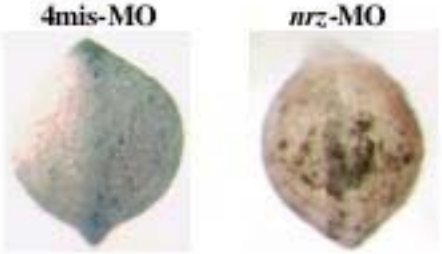

Figure 4D

E

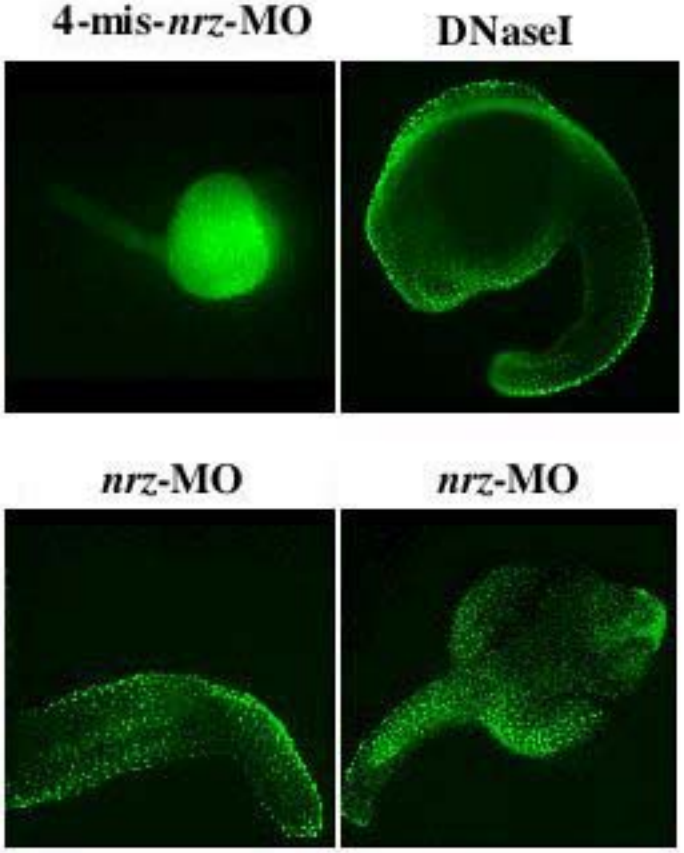

Figure 4E

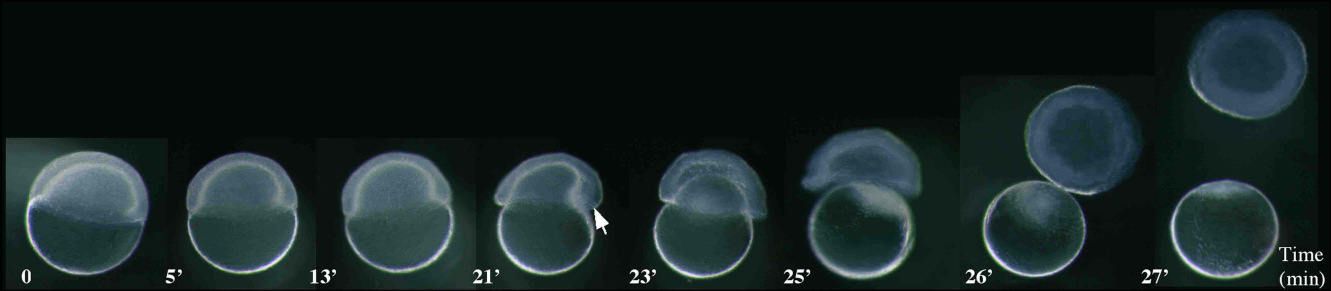
0
5'
13'
21'
23'
25'
26'
27'
Time
(min)

A

4mis-MO

nrz-MO

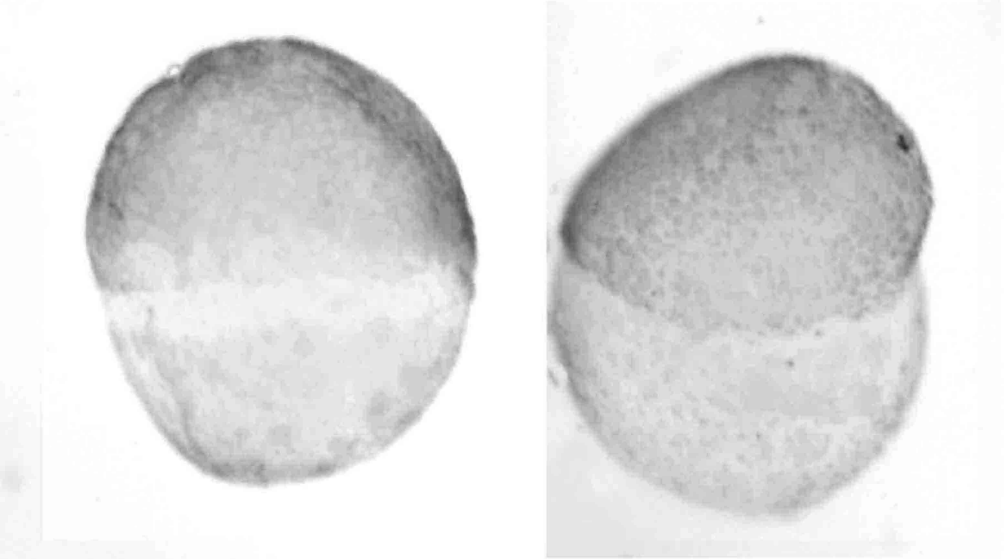

B

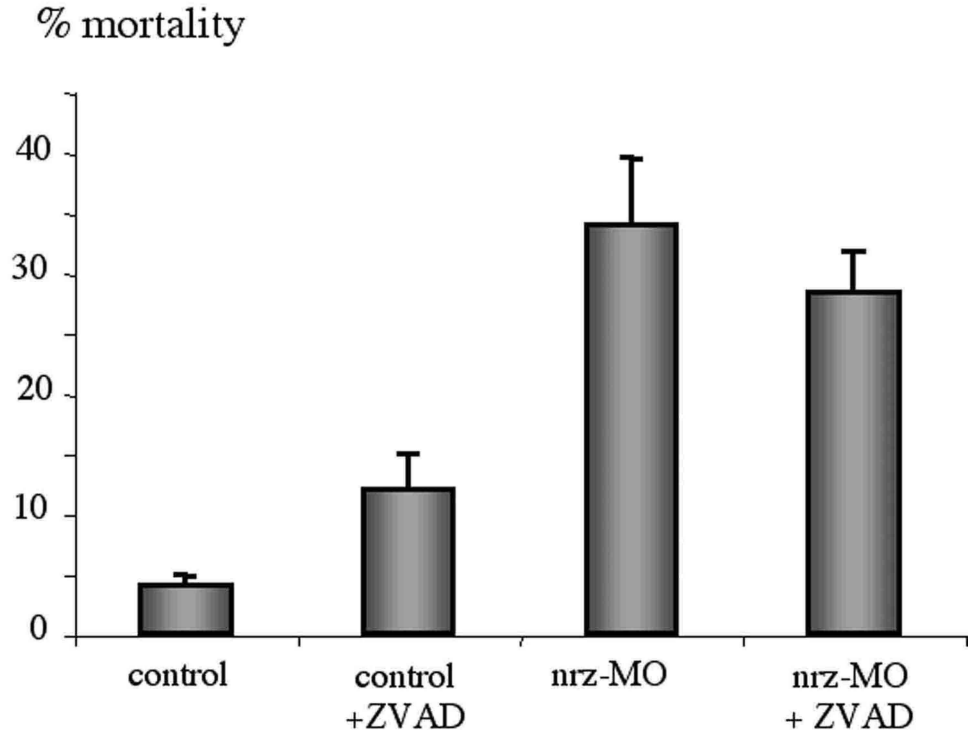

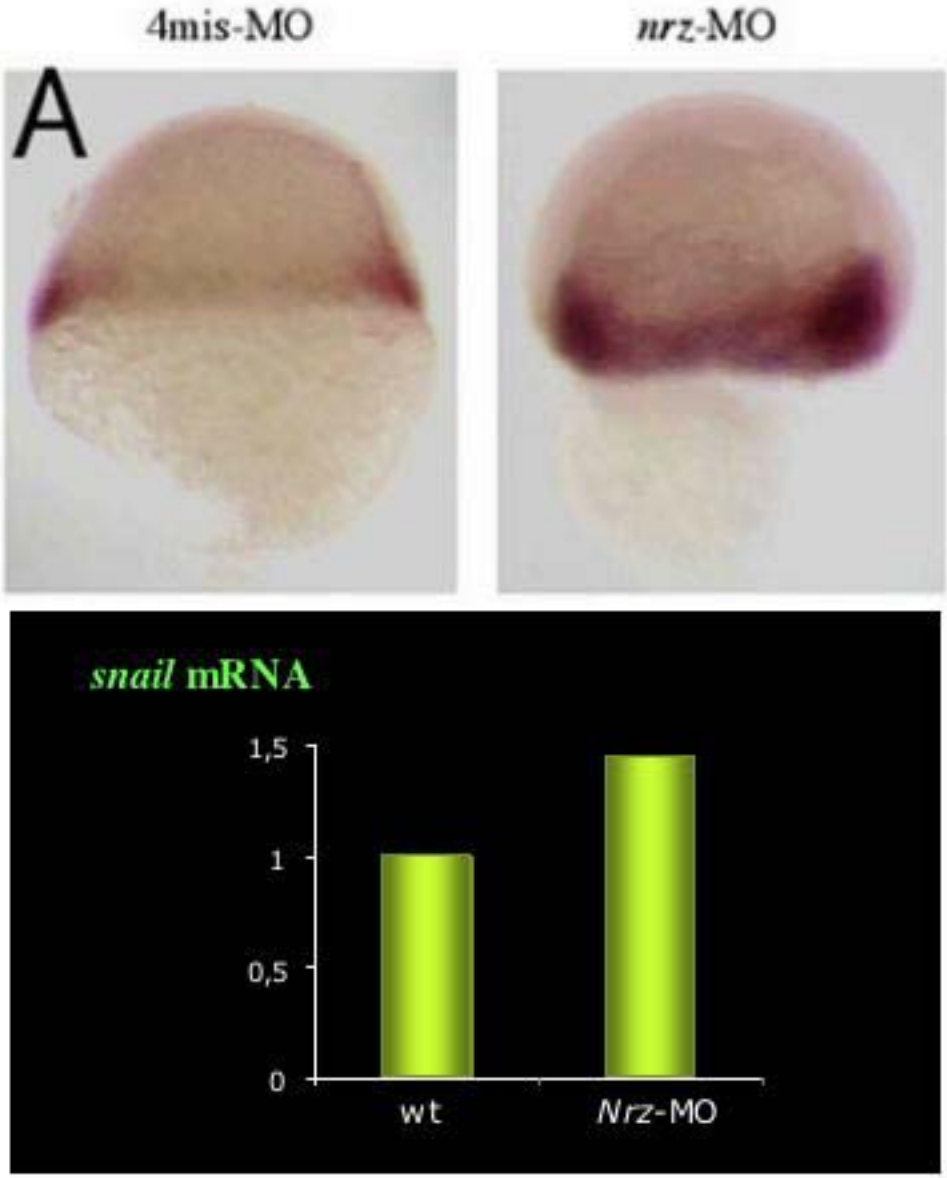

Figure 7A

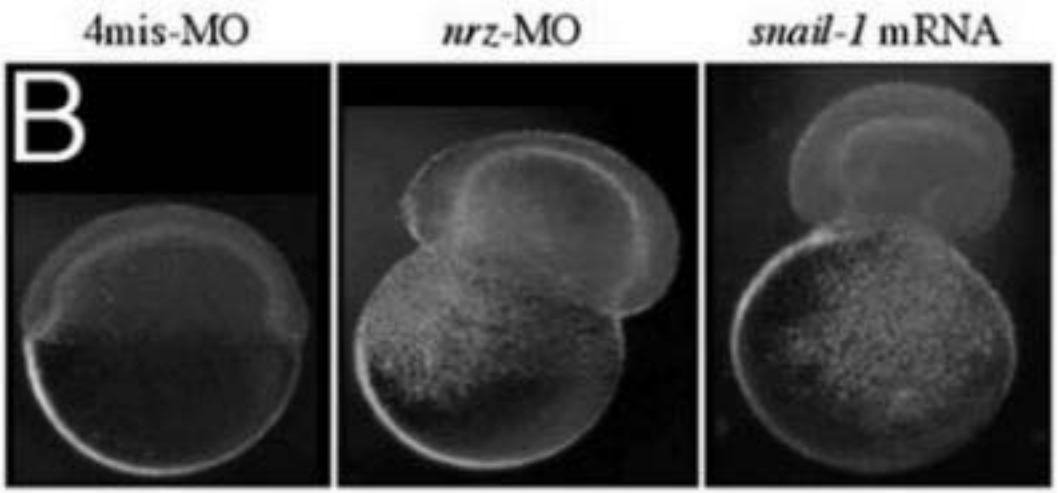

Figure 7B

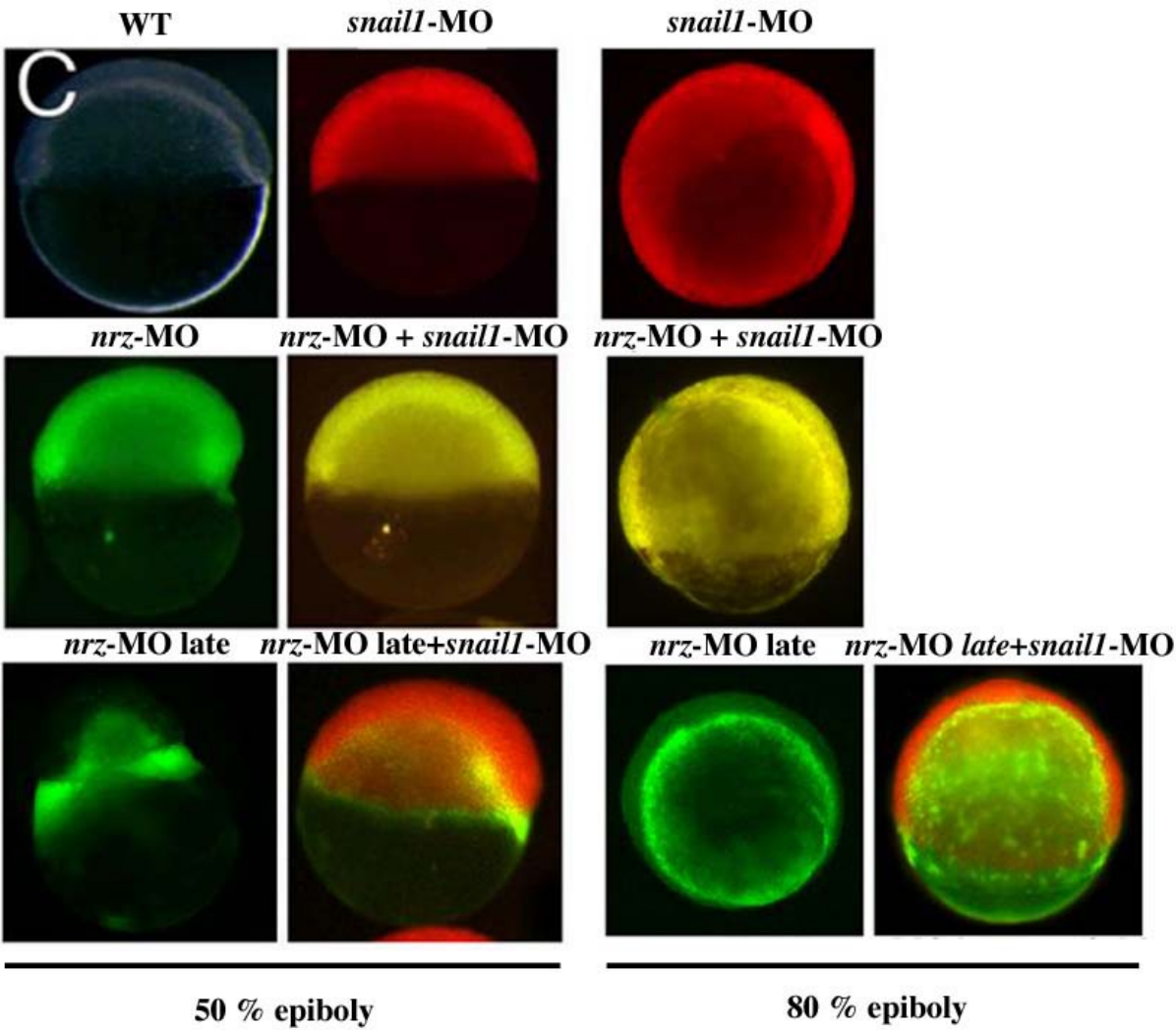
WT
snail1-MO
snail1-MO
C
nrz-MO
nrz-MO + snail1-MO
nrz-MO + snail1-MO
nrz-MO late
nrz-MO late+snail1-MO
nrz-MO late
nrz-MO late+snail1-MO
50 % epiboly
80 % epiboly

Figure 7C

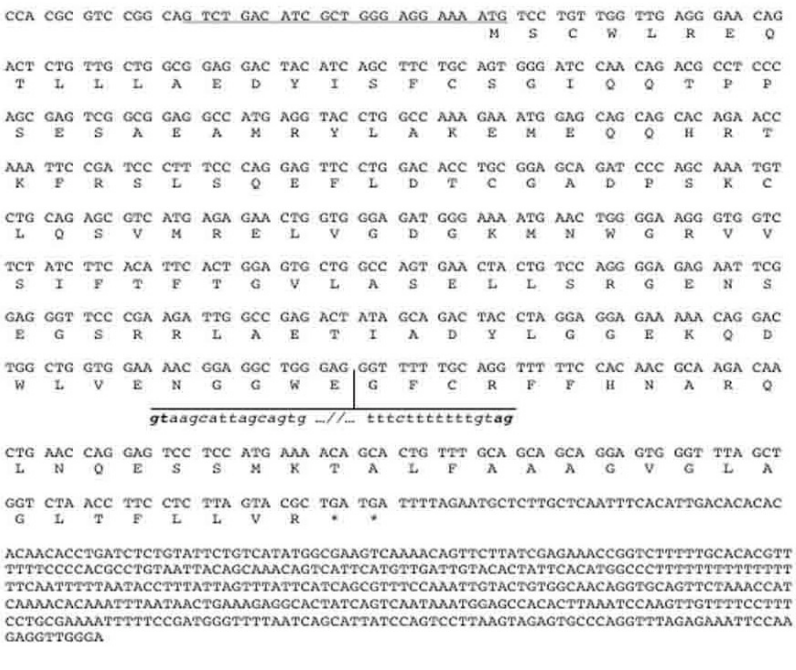

Genomic organization of nrz. The deduced amino acid sequence is shown.
The position of the intron is indicated (italics).
The antisense morpholino nrz-MO hybridizes with the underlined sequence close to the ATG.

Injection of *snail1* mRNA (Time Lapse)

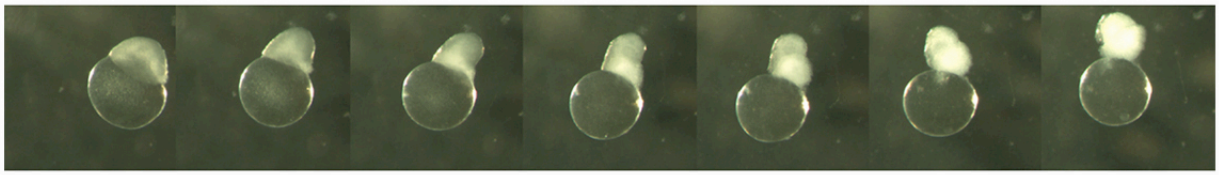

Time (min)	0	16	28	32	35	38	40

Effect of the injection of *snail1* mRNA on gastrulation. Video time lapse analysis. Embryos were injected at stage 1-4 cells.
The video sequence shown starts before the 50% epiboly stage (time 0). Progression of the margin is arrested and cells of the animal pole detach from the yolk syncitial layer. This phenotype is very similar to *nrz* morphants (see Fig. 5)

*papc*ISH

4mis-*nrz*-MO

nrz-MO

Expression of the paraxial protocadherin (PAPC) as detected by whole mount in situ hybridieation in zebrafish embryos (epiboly stage) injected with either the nrz antisense (nrz-MO, bottom) or the negative control (4mis, top). Expression of PAPC at the margin is apparently higher in nrz morphants.